PHYSICAL REVIEW B **73**, 214405 (2006)

Condensation of magnons and spinons in a frustrated ladder

J.-B. Fouet
Institut Romand de Recherche Numérique en Physique des Matériaux (IRRMA), PPH-Ecublens, CH-1015 Lausanne, Switzerland

F. Mila
Institute of Theoretical Physics, École Polytechnique Fédérale de Lausanne, CH-1015 Lausanne, Switzerland

D. Clarke, H. Youk, and O. Tchernyshyov
Department of Physics and Astronomy, Johns Hopkins University, 3400 North Charles Street, Baltimore, Maryland 21218, USA

P. Fendley
Department of Physics, University of Virginia, Charlottesville, Virginia 22904-4714, USA

R. M. Noack
Fachbereich Physik, Philipps Universität Marburg, D-35032 Marburg, Germany
(Received 24 March 2006; published 6 June 2006)

Motivated by the ever-increasing experimental effort devoted to the properties of frustrated quantum magnets in a magnetic field, we present a careful and detailed theoretical analysis of a one-dimensional version of this problem, a frustrated ladder with a magnetization plateau at $m=1/2$. We show that even for purely isotropic Heisenberg interactions, the magnetization curve exhibits a rather complex behavior that can be fully accounted for in terms of simple elementary excitations. The introduction of anisotropic interactions (e.g., Dzyaloshinskii-Moriya interactions) modifies significantly the picture and reveals an essential difference between integer and fractional plateaus. In particular, anisotropic interactions generically open a gap in the region between the plateaus, but we show that this gap closes upon entering fractional plateaus. All of these conclusions, based on analytical arguments, are supported by extensive density matrix renormalization group calculations.

DOI: 10.1103/PhysRevB.73.214405 PACS number(s): 75.10.Jm, 75.10.Pq, 75.40.Mg, 75.30.Kz

I. INTRODUCTION

Quantum phase transitions[1] occur when the variation of an external parameter (pressure, chemical composition, etc.) produces a singular change of a system's ground state. If the transition is continuous, the properties of the system in the vicinity of the quantum critical point are dominated by universal features, which can be described in field-theoretic language.[1] Quantum phase transitions and related critical behavior are observed in a variety of physical systems, from heavy-fermion compounds[2] to quantum magnets[3] and cold atomic gases.[4]

In antiferromagnets the external parameter is typically an applied magnetic field $\mathbf{H}=(0,0,H)$. If the longitudinal component of the total spin, S^z, is a good quantum number, the magnetic moment of the ground state $M=g\mu_B\langle S^z\rangle$ as a function of H may exhibit several plateaus, on which $dM/dH=0$, separated by regions of continuously varying magnetization. The ends of a plateau are quantum critical points separating an incompressible ground state with an energy gap from a compressible state with gapless excitations. Affleck[5] noted in the context of spin 1 chains that such a phase transition is similar to the condensation in a system of interacting bosons, a point of view reemphasized and extended in the context of coupled spin 1/2 ladders.[6] The magnetic field and magnetic moment play the roles of the chemical potential and particle number. The condensing objects are magnons, the quasiparticles carrying spin $\Delta S^z=\pm 1$. The field theory describing the bosons near the Bose-condensation point[7] is equally applicable to the end points of a magnetic plateau.

Not every magnetization plateau ends in a simple condensation of magnons. If the plateau state breaks a symmetry of the lattice while the gapless state does not, the transition must restore the broken lattice symmetry. The universal properties of such a transition are expected to be different. In one spatial dimension, the picture based on the magnon condensation is generally applicable to "integer" magnetization plateaus defined as follows:[8] the spin per unit cell differs from the maximal value by an integer. A fractional magnetization plateau may end in a phase transition belonging to a different universality class. Examples of such behavior were recently discussed by a number of authors.[9–11]

In this paper, we present a theoretical study of quantum phase transitions in a one-dimensional model antiferromagnet exhibiting both integer and fractional magnetization plateaus. We employ numerical methods to observe critical behavior and compare the results to predictions of the appropriate field theories. The outcome of our work stresses the importance of anisotropic interactions in the vicinity of quantum critical points, a point raised by previous authors.[12,13] Even a weak anisotropy makes a significant impact on the quantum phase transitions in question and, furthermore, the effects vary substantially between different universality classes.

The paper is organized as follows. The model system and details of the numerical method are described in Sec. II. In Sec. III we discuss the ground states and phase transitions in

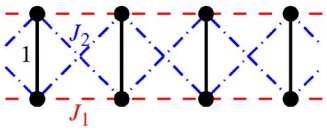

FIG. 1. (Color online) The frustrated ladder. The exchange couplings are set to 1 on the vertical rungs, $J_1=0.55$ on horizontal legs, and $J_2=0.7$ on the diagonals.

the model with isotropic interactions. The influence of anisotropy is the subject of Sec. IV and a summary of the results is given in Sec. V.

II. DESCRIPTION OF THE MODEL

A. Hamiltonian and ground states

Our model system is the frustrated ladder with spin-1/2 spins and with Heisenberg exchange.[14] The largest exchange couplings, of strength 1, are on the rungs, with somewhat weaker couplings J_1 along the legs and J_2 along plaquette diagonals, see Fig. 1. The Hamiltonian is

$$\mathcal{H} = \sum_{n=1}^{L} [\mathbf{S}_{n,1}\cdot\mathbf{S}_{n,2} - H(S^z_{n,1}+S^z_{n,2})] + J_1\sum_{n=1}^{L-1}(\mathbf{S}_{n,1}\cdot\mathbf{S}_{n+1,1}+\mathbf{S}_{n,2}\cdot\mathbf{S}_{n+1,2}) + J_2\sum_{n=1}^{L-1}(\mathbf{S}_{n,1}\cdot\mathbf{S}_{n+1,2}+\mathbf{S}_{n,2}\cdot\mathbf{S}_{n+1,1}). \quad (1)$$

A ladder without diagonal links ($J_2=0$) was examined in Ref. 15. The point $J_1=J_2$ is special: the spin of each rung is a conserved quantity and the ground state is known exactly.[16] Conditions for the existence of a $m=1/2$ plateau in the general case were given in Ref. 14.

In this work, we study the case where the interrung couplings J_1 and J_2 are nonvanishing and similar in strength. Proximity to the exactly solvable model $J_1=J_2$ suggests a partition of the Hamiltonian into an exactly solvable part plus a small perturbation. To that end, it is convenient to introduce the operators of the total spin of a rung $\mathbf{S}_n=\mathbf{S}_{n,1}+\mathbf{S}_{n,2}$ and the spin difference $\mathbf{D}_n=\mathbf{S}_{n,1}-\mathbf{S}_{n,2}$. The exchange part of the Hamiltonian is then a sum of three terms:

$$\mathcal{H}_0 = \sum_{n=1}^{L}(\mathbf{S}_n)^2/2 - HS^z_n, \quad \mathcal{H}_1 = J\sum_{n=1}^{L-1}\mathbf{S}_n\cdot\mathbf{S}_{n+1},$$

$$\mathcal{H}_2 = \frac{\delta J}{2}\sum_{n=1}^{L-1}\mathbf{D}_n\cdot\mathbf{D}_{n+1}, \quad (2)$$

where $J=(J_1+J_2)/2$ and $\delta J=J_1-J_2$. The algebra of **D** operators is discussed in Appendix A.

The physics of the model is rather simple when the energy scales are well separated,

$$\delta J \ll J \ll 1. \quad (3)$$

The dominant term $\mathcal{H}_0$ favors a spin singlet on every rung at low fields $H<1$ as depicted in Fig. 2(a). In high fields, $H>1$, the state of lowest energy is the $S^z=+1$ component of the triplet. (The other two components of the triplet are high-energy states in any magnetic field.) The all-singlet and all-triplet states are the origins of the two *integer* magnetization plateaus with the spin per rung $m=S^z/L=0$ and 1, respectively.

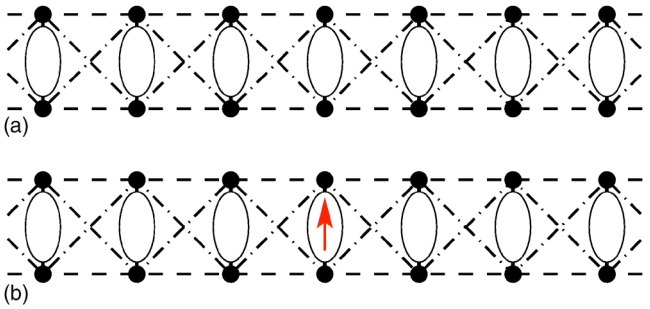

FIG. 2. (Color online) (a) A sketch of the ground state at low magnetic fields: all of the rungs are in the $S=0$ state. (b) Elementary excitations out of this state are magnons carrying spin $\Delta S^z=+1$.

The next term $\mathcal{H}_1$ represents a repulsion between triplets on neighboring rungs. This repulsion does not allow the triplets to condense on all rungs at once and introduces an intermediate, *fractional* magnetization plateau with a triplet on every other rung and spin per rung $m=1/2$. Accordingly, there are two ground states breaking the translational symmetry, illustrated in Figs. 3(a) and 3(b), which we refer to as the Néel states. The fractional plateau exists in the range of fields $1<H<1+2J$.

Finally, the smallest term $\mathcal{H}_2$ endows the triplets with mobility: unlike the total spin of the rung $\mathbf{S}_n$, the spin difference $\mathbf{D}_n$ does not commute with the dominant term $\mathcal{H}_0$. The

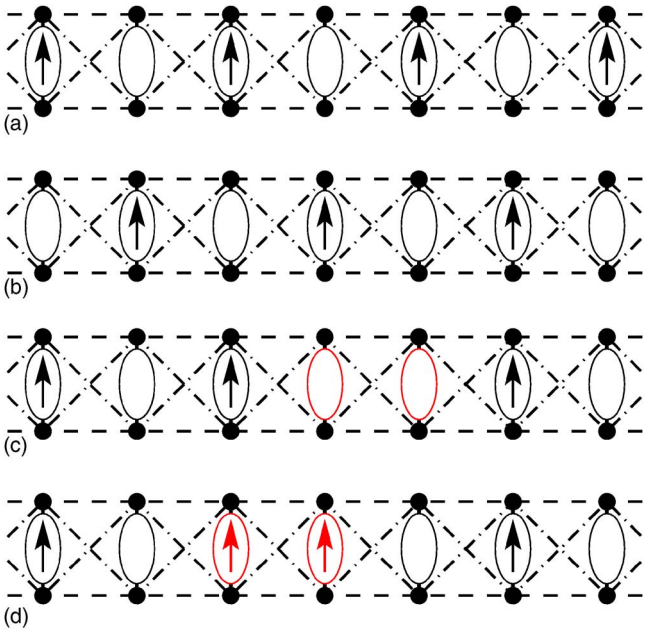

FIG. 3. (Color online) (a) and (b) depict the two ground states of the fractional plateau with Z_2 translational order. Elementary excitations are domain walls carrying $S^z=-1/2$ at (c) the low-field end of the plateau and $S^z=+1/2$ at (d) the high end.

triplets acquire a kinetic energy of the order δJ. As a result, the fractional and integer plateaus become separated by gapless phases with a constantly varying magnetization and with spin correlations that decay as a power of the distance between sites.

The resulting Hamiltonian (2) has an axial $O(2)$ symmetry. However, in real materials that symmetry is often violated by small additional interactions induced by the relativistic spin-orbital coupling. In many cases such interactions act like a staggered transverse magnetic field.[12,13] We consider the influence of such additional terms in Sec. IV.

B. Elementary excitations

At the end of the $m=0$ plateau, the elementary excitations are individual triplets carrying spin $\Delta S^z=+1$ [Fig. 2(b)]. Similarly, low-energy excitations near the end of the $m=+1$ plateau are isolated singlets in the background of $S^z=+1$ triplets. They carry spin $\Delta S^z=-1$. We refer to both of these excitations as *magnons.*

The low-energy excitations near the ends of the fractional plateau are domain walls with spin $\Delta S^z=-1/2$ at the lower-field end and $\Delta S^z=+1/2$ at the high-field end [Figs. 3(c) and 3(d)]. They will be referred to as *spinons.* The quantum phase transitions between the plateaus and gapless phases are triggered by the condensation of these elementary excitations.

C. Mapping onto an *XXZ* spin chain, hard-core bosons, and fermions

In the regime described by Eq. (3), each rung can be found either in the singlet or in the $S^z=+1$ triplet state. Effectively, we can treat this as a system with only two states per site, using perturbation theory in δJ to define a Hamiltonian that acts on this reduced Hilbert space.

By identifying the singlet and the $S^z=1$ triplet states with the spin-up and spin-down states, respectively, we map the ladder onto a spin-1/2 *XXZ* antiferromagnetic chain with an easy-axis anisotropy.[14] Defining the usual spin-1/2 matrices s^x, s^y, and s^z acting on the reduced Hilbert space, one has

$$\mathcal{H}_{xxz} = \sum_{n=1}^{L-1} [j_x(s_n^x s_{n+1}^x + s_n^y s_{n+1}^y) + j_z s_n^z s_{n+1}^z] - H_{\text{edge}}(s_1^z + s_L^z)/2 - H_{xxz}\sum_{n=1}^{L} s_n^z, \quad (4)$$

where

$$j_x = \delta J + O(\delta J^2), \quad j_z = J + O(\delta J^2),$$

$$H_{xxz} = H - 1 - J + O(\delta J^2). \quad (5)$$

The additional magnetic field $H_{\text{edge}}=J$ at the chain ends breaks the symmetry between the two Néel states of this effective spin chain. The edge field plays a role in the formation of the ground state at the fractional plateau, where singlets and $S^z=+1$ triplets have comparable energies.

The *XXZ* chain is gapped in the antiferromagnetic regime $j_z/|j_x|>1$ and $H_{xxz}=0$, with zero magnetization in the ground state.[17] The presence of the energy gap means that the magnetization remains exactly zero in a finite range of fields $-H_{\min}<H_{xxz}<H_{\min}$. At $\pm H_{\min}$ the energy gap vanishes and the spinons condense. (The corresponding fields in the ladder correspond to the edge of the $M=1/2$ plateau and are called H_{c3} and H_{c2}, respectively.) As $|H_{xxz}|$ is increased further, the ground state becomes a sea of spinons with a growing magnetization. The system in this regime is a Luttinger liquid with continously varying critical exponents.[18] Finally, at $H_{xxz}=\pm H_{\max}$ the magnetization of the *XXZ* chain saturates (in the ladder, this corresponds to the saturation field H_{c4} and to the field H_{c1} at the end of the $m=0$ plateau). The critical fields of the *XXZ* chain are known exactly:[17]

$$H_{\max} = j_z + |j_x|, \quad H_{\min} = |j_x| \sinh g \sum_{n=-\infty}^{\infty} \frac{(-1)^n}{\cosh ng}, \quad (6)$$

where $\cosh g = j_z/|j_x|$.

The system can also be viewed as a one-dimensional hard-core Bose gas: the singlet state of a rung is mapped onto an empty site, and a $S^z=+1$ triplet becomes an occupied site. The bosons have hopping amplitude $\delta J/2$, strong nearest-neighbor repulsion J, and chemical potential H_{xxz}.

In one dimension, the hard-core constraint can be removed by replacing the bosons with spinless fermions. This representation is particularly convenient when the Bose system is nearly empty ($m \ll 1$) or nearly filled ($1-m \ll 1$). In these limits, the short-range repulsion between the fermions is largely suppressed by the Pauli principle. Near the fractional plateau, when $|m-1/2| \ll 1$, it is convenient to represent the domain walls as spinless fermions.[19]

D. Numerical work

When the energy scales do not form the hierarchy of Eq. (3), one must resort to numerical methods. Nonetheless, the general picture painted above remains largely intact and, furthermore, the critical behavior near the quantum phase transitions is expected to be universal. To verify this, we have numerically determined the ground state, its magnetization, and the energy gap in a ladder with coupling constants $J_1=0.55$ along the legs and $J_2=0.7$ along the plaquette diagonals. The ground and first excited states were determined by the density matrix renormalization group (DMRG) method.[20] We have worked with ladders with up to 200 rungs, and have used the so-called "finite algorithm" version of the DMRG method.[21] The use of open boundary conditions allows us to study oscillations of magnetization $\langle S_n^z \rangle$ induced by the presence of the ends.

For the model with isotropic interactions, we have carried out two sweeps and have retained $m=600$ states in the system block. The typical weight of discarded density-matrix eigenvalues is of order 10^{-12}. We have performed a few calculations with six sweeps and $m=1000$ states; the energy difference was of the order of 10^{-7}. We have calculated the ground state in each S_z sector in zero magnetic field for sizes up to $N=400$ and by comparing energies in a field have deduced the global ground state as a function of magnetic field.

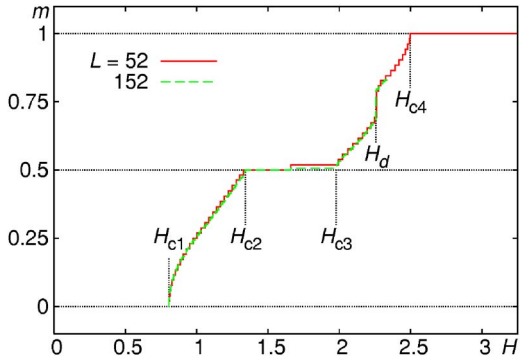

FIG. 4. (Color online) Magnetization per rung $m=\langle S^z\rangle/L$.

For the model with a staggered field, S_z is no longer a good quantum number, and we need to make a calculation for each value of the magnetic field H. Fortunately, due to the opening of the gap, far fewer states are needed: carrying out two sweeps and keeping only $m=200$ states for up to $N=200$ sites and $m=400$ for larger systems, the typical discarded weight was of order 10^{-11}.

The other subtle issue when performing DMRG simulations is the choice of boundary conditions. Since one cannot access all excited states with the DMRG, choosing the appropriate boundary conditions can be crucial to obtaining relevant information about the excitation gap.

In the case of an isotropic chain, for which the gap is not an issue, we have worked with open boundary conditions. As a result, in the $m=1/2$ plateau the ladder with an even number of rungs L has a single spinon in the ground state (see Sec. III B 2 for details). The small magnetization step in the middle of the fractional plateau occurs when the spinon changes its spin from $\Delta S^z=-1/2$ to $+1/2$.

For systems with a staggered field, however, we have used asymmetric boundary conditions, imposing different values of the rung couplings at the edge: $J=1.8$ for the first rung and $J=0.2$ for the last one. These boundary conditions are necessary for the determination of the energy gap in the formerly gapless regime between H_{c1} and H_{c2} (Fig. 4). With open boundary conditions, the system has two nearly degenerate ground states. Altering the end rungs as described above lifts this near-degeneracy and pushes one of the ground states well above the first excited state.

III. LADDER WITH ISOTROPIC INTERACTIONS

In this section, we present a detailed analysis of the properties of the frustrated ladder without anisotropic interactions. The basic properties of this system have been described before.[14–16] In particular, the magnetization curve is expected to have plateaus at $m=0$, $m=1/2$, and $m=1$, to increase monotonically between the plateaus, and to have square-root singularities at all plateau ends. In practice, the magnetization curve differs from the naive expectations in a number of ways. For example, the square-root singularity in the magnetization near the fractional plateau is barely detectable; a jump in magnetization is seen in the gapless region between the $m=1/2$ and $m=1$ plateaus; the magnon mass near H_{c1} differs significantly from the prediction of perturbation theory. We discuss the main features of the magnetization curve below.

A. Critical points

The results for $L=52$ and 152 rungs are shown in Fig. 4. As expected, the magnetization curve has three plateaus at $m=0$, $1/2$, and 1. The $m=0$ plateau ends at $H_{c1}=0.806$, the $m=1/2$ plateau lies between $H_{c2}=1.345$ and $H_{c3}=1.974$, and a fully polarized state with $m=1$ begins at $H_{c4}=2.500$. A finite jump in the magnetization $\Delta m=0.099$ is observed in a compressible regime at $H_d=2.254$. We next discuss the critical fields.

1. Magnon condensation at H_{c4}

It is straightforward to calculate the end point of the fully polarized state $m=1$. When the energy scales separate well, i.e., in the regime described by Eq. (3), the excitations with the lowest energies are singlets with the dispersion

$$\epsilon_{0,0}(k) = H - 1 - 2J + \delta J \cos k. \tag{7}$$

The singlets are gapped in fields $H > H_{0,0} = 1 + 2J + |\delta J| = 2.4$ for our choice of couplings. However, the numerics show that the condensation occurs at a somewhat higher field. This discrepancy can be traced to a poor separation of energy scales: $J=0.625$ is not that small. As a result, the first excitations to condense are the $S^z=0$ components of the triplet, whose energy dispersion is

$$\epsilon_{1,0}(k) = H - 2J + 2J \cos k, \tag{8}$$

and the condensation field $H_{1,0}=4J=2.5$, in perfect agreement with the numerics.

2. Spinon condensation at H_{c2} and H_{c3}

To lowest order in δJ, the end points of the fractional plateau $m=1/2$ can be obtained in a similar way. The spinons carrying $S^z=\pm 1/2$ have energies

$$\epsilon_{-1/2}(k) = (H-1)/2 + \delta J \cos 2k + O(\delta J^2),$$

$$\epsilon_{+1/2}(k) = (1-H)/2 + J + \delta J \cos 2k + O(\delta J^2). \tag{9}$$

These spinons condense at

$$H_{c2} \approx 1 + 2|\delta J| = 1.3 \quad \text{and} \quad H_{c3} \approx 1 + 2J - 2|\delta J| = 1.95, \tag{10}$$

respectively, which are not that far off from the values $H_{c2}=1.345$ and $H_{c3}=1.974$ obtained from the DMRG.

To improve the lowest-order estimate, we have expanded the parameters of the XXZ chain (5) and its critical field $H_{\min}$ (6) to $O(\delta J^2)$. The physical origin of these corrections can be traced to quantum fluctuations of spins in the ground and excited states of the $m=1/2$ plateau and its excitations. The term $\mathcal{H}_2$ in the Hamiltonian connects the $S^z=-1/2$ spinon [two adjacent singlets, see Fig. 3(c)] to high-energy states, shifting its energy by an amount $C\delta J^2<0$. The energy of the

$S^z=+1/2$ spinon [Fig. 3(d)] is unaffected by quantum fluctuations at this order.

The energy shift of the $S^z=-1/2$ spinon can be taken into account by adding the following term to the Hamiltonian of the *XXZ* chain:

$$\Delta\mathcal{H}_{XXZ} = \sum_n (1/2 - s_n^z)(1/2 - s_{n+1}^z) C\delta J^2$$

$$= \text{const} - C\delta J^2 \sum s_n^z + C\delta J^2 \sum s_n^z s_{n+1}^z. \quad (11)$$

It can be seen that the added term affects both the Ising coupling and the effective field of the *XXZ* chain:

$$j_x = \delta J + O(\delta J^3), \quad j_z = J + C\delta J^2 + O(\delta J^3),$$

$$H_{xxz} = H - 1 - J + C\delta J^2 + O(\delta J^3). \quad (12)$$

Expansion of Eq. (6) in powers of δJ yields the lower critical field of the *XXZ* chain

$$H_{\min} = J - 2|\delta J| + (C + 1/2J)\delta J^2 + O(\delta J^3). \quad (13)$$

The resulting condensation point of the $S^z=+1/2$ spinons

$$H_{c3} \approx 1 + 2J - 2|\delta J| + \delta J^2/2J = 1.968 \quad (14)$$

is now very close to the DMRG value of 1.974.

The critical field of the $S^z=-1/2$ spinons is sensitive to the energy shift $C\delta J^2$. The function $C(J)$ is computed in Appendix B. For $J=0.625$ we obtain $C=-2.026$ and thus

$$H_{c2} \approx 1 + 2|\delta J| - (2C + 1/2J)\delta J^2 = 1.374. \quad (15)$$

Comparing it to the DMRG value of 1.345, we see only a modest improvement over the first-order result (10). The apparent reason for the slow convergence of the perturbation series for H_{c2} is the fairly small energy gap ($\Delta=0.255$) separating the $S^z=-1/2$ spinons from higher-energy states (see Appendix B).

3. Magnetization jump at $H_d=2.254$

Between H_{c3} and H_{c4}, the ground state switches from a mixture of $S^z=+1$ triplets and singlets to one of $S^z=+1$ and $S^z=0$ triplets. This transition is accidental in the sense that it is not accompanied by any change in symmetry. It is therefore not surprising that the change is accompanied by a discontinuity in the magnetization.

4. Magnon condensation at H_{c1}

The energy of an isolated $\Delta S^z=1$ excitation at the $m=0$ plateau is

$$\epsilon_{1,1}(k) = 1 - H + \delta J \cos k + O(\delta J^2). \quad (16)$$

Thus, to first order in δJ, the magnon condensation is expected at $H_{c1}=1-|\delta J|=0.85$, not very far from the DMRG result 0.806.

At $O(\delta J^2)$ quantum fluctuations not only lower the energy of the magnon but also change its hopping amplitude (Fig. 5). The magnitude of the second-order correction is rather large, again thanks to a small energy gap ($\Delta=0.125$) between the magnon and higher-energy states. See Appendix C for details.

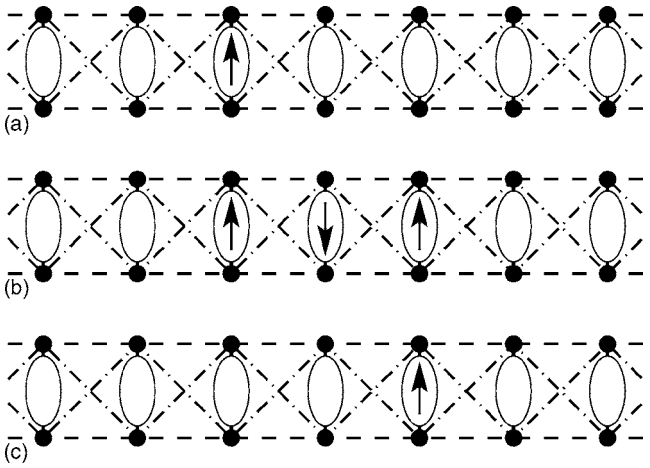

FIG. 5. Corrections to the kinetic energy of a magnon at the order δJ^2: (a)→(b) A pair of triplet states with net spin zero is created adjacent to an existing magnon. (b)→(c) One of those triplet states annihilates with the original magnon, leaving a new magnon on a different lattice site. This process provides an additional channel for magnon motion and thus lowers the effective magnon mass.

B. Magnetization patterns

Thanks to the presence of an energy gap, both the total spin S^z and the average spin of an individual rung $\langle S_n^z\rangle$ remain exactly zero in the low-field regime $|H|<H_{c1}$. As the field increases beyond H_{c1}, both the local and the total spin begin to increase. In a finite ladder, the local magnetization $\langle S_n^z\rangle$ is distributed in a nonuniform way, revealing interference patterns.

1. $m \ll 1$: dilute magnons

At low concentrations, the magnetization is carried by individual magnons which can be viewed as hard-core bosons or, more conveniently, as free fermions with spin $\Delta S^z=+1$. (The nearest-neighbor repulsive potential acting between magnons is rendered irrelevant by the Fermi statistics.) Treating the magnons as ideal fermions one obtains a magnetization distribution

$$\langle S_n^z\rangle = \sum_{k=1}^{S^z} |\psi_k(n)|^2, \quad (17)$$

where, in the continuum approximation, $\psi_k(n) = \sqrt{2/L}\sin(\pi k n/L)$ is the wave function of a nonrelativistic fermion in a box of length $L+1$. This simple model agrees well with the magnetization distribution obtained numerically at small values of the magnetization $m=S^z/L$ (Fig. 6). Deviations already become noticeable when m reaches $1/20$.

The free-fermion approach predicts a fast initial growth of magnetization $m=S^z/L$:

$$m \sim \Delta S^z k_F/\pi = \pi^{-1}|\Delta S^z|^{3/2}\sqrt{2m^*|H - H_{c1}|}, \quad (18)$$

where the inverse mass $1/m^* \approx |\delta J|$. We have found numerically that m^2 indeed rises linearly with H (Fig. 7). However,

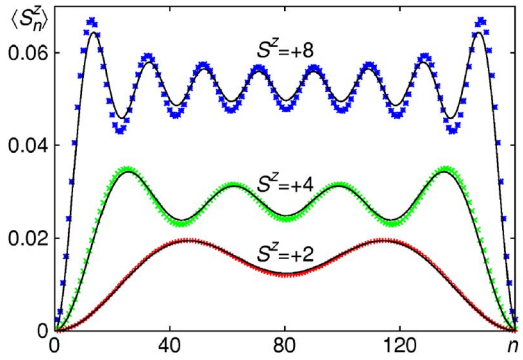

FIG. 6. (Color online) Distribution of spin $\langle S_n^z \rangle$ as a function of rung position n in the ground state off of the $m=0$ plateau. The symbols are the numerical results at $S^z=2$, 4, and 8. The curves are spin distributions for 2, 4, and 8 magnons treated as free fermions carrying spin $\Delta S^z=+1$. Calculations are on a ladder with $L=160$ rungs.

the slope dm^2/dH is less than a third of the calculated value of $2\pi^{-2}|\delta J|^{-1}$.

To track down the source of the discrepancy, we have computed the contribution of higher-order processes to the magnon dispersion. The $O(\delta J^2)$ term turns out to be *larger* than the first-order result. This can be understood on a qualitative level by considering a typical $O(\delta J^2)$ contribution to the kinetic energy of the magnon in which two additional magnons are created and destroyed (Fig. 5). The lowest-lying 3-magnon state has an energy of $\Delta=2-3J$ above that of a single magnon. For $J=0.625$, this energy gap $\Delta=0.125$ is comparable to the small parameter $\delta J=-0.15$, meaning that the lowest-order perturbation theory in δJ may not give reliable results. See Appendix C for details.

2. $|m-1/2| \ll 1$: *dilute spinons*

The numerically determined distribution of magnetization $\langle S_n^z \rangle$ exactly at $m=1/2$ ($S^z=80$ in a ladder with $L=160$ rungs) is shown in Fig. 8(a). Contrary to our initial expectations, the plateau state is *not* a simple Néel state with a constant staggered magnetization on top of a constant background $1/2+(-1)^n/2$. The staggered magnetization is highly nonuniform.

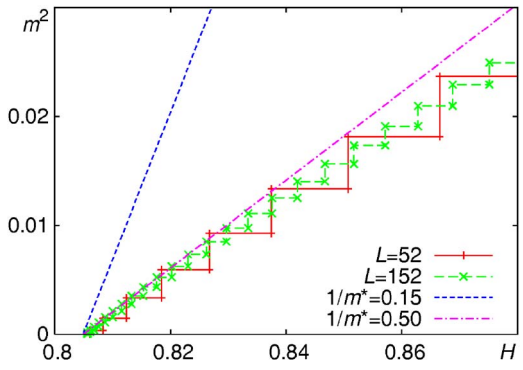

FIG. 7. (Color online) The square of magnetization density m off the $m=0$ plateau.

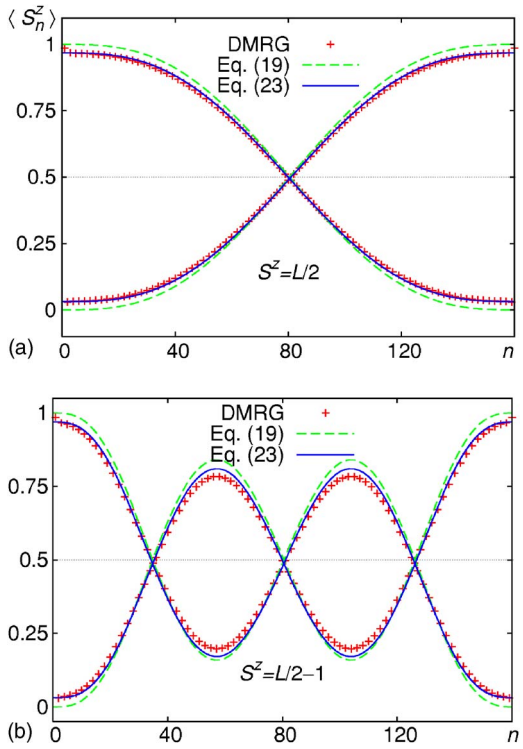

FIG. 8. (Color online) Distribution of magnetization $\langle S_n^z \rangle$ in a ladder with $L=160$ rungs. (a) Exactly at the magnetization plateau $m=1/2$, or $S^z=L/2$, the ladder contains one spinon. (b) At $S^z=L/2-1$, three spinons are present.

To understand this result, consider the $m=1/2$ plateau state in a finite ladder with an even number of rungs L. To $O(\Delta J^0)$, its ground states are configurations with $L/2$ triplets with no two triplets next to each other. There are only two such states in a ladder with periodic boundary conditions. In contrast, for open boundary conditions there are $L/2+1$ such configurations: two Néel states and $L/2-1$ states with a singlet-singlet domain wall (Fig. 9). The term $\mathcal{H}_2$ delocalizes the domain wall and is ultimately responsible for the strong modulation of the staggered magnetization.

The mapping onto the *XXZ* chain provides an alternative perspective. Ordinarily, the two Néel states of the *XXZ* chain are degenerate even in the presence of a uniform magnetic field. However, our system (4) has an extra magnetic field of strength $-J/2$ at the ends, so that both end spins prefer the $+1/2$ state. In a chain of even length, this inevitably leads to the formation of a domain wall. The cost of the wall $(+J/2)$ is exactly offset by the reduction of the energy of the end spin $(-J/2)$; a negative delocalization energy of the domain wall $(-|\delta J|)$ lowers the energy of this state relative to the Néel state. Thus the effective *XXZ* chain always has spins $+1/2$ at the ends in this regime. Accordingly, the end rungs of the ladder are in the triplet state and thus there must be a single domain wall somewhere in the chain.

The strong modulation of the staggered magnetization evident in Fig. 8(a) can be traced to the delocalization of the spinon. Rung n is in the state with spin $S=1/2-(-1)^n/2$ if the domain wall is on its right, otherwise it has spin $S=1/2+(-1)^n/2$. For a rung near the left edge, the domain

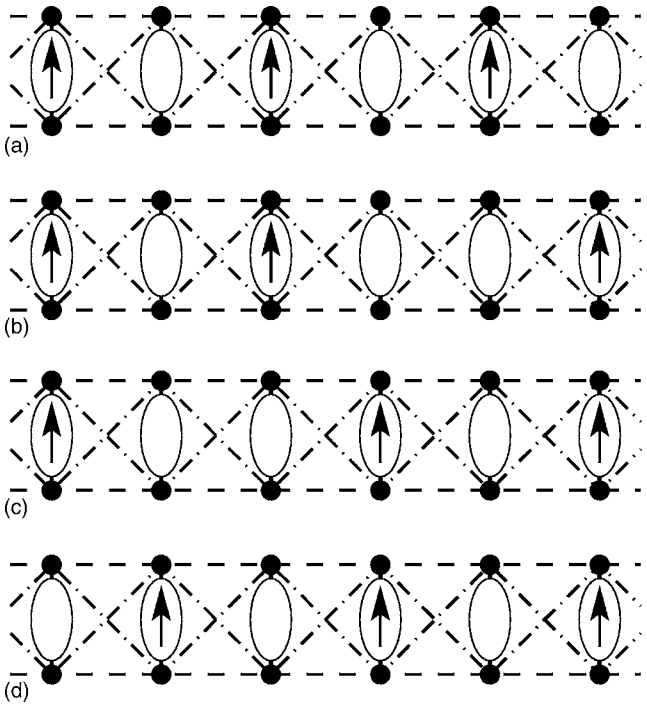

FIG. 9. Low-energy states of a ladder with an even number of rungs at magnetization density $m=1/2$.

wall is almost always on the right and vice versa. Thus we expect

$$\langle S_n^z \rangle = \frac{1}{2} - \frac{(-1)^n E(n)}{2}, \tag{19}$$

where the smooth envelope $E(n)$ interpolates between +1 and −1 and has a node in the middle.

To evaluate the envelope $E(n)$, we adopt the continuum approximation and treat the spinon as a nonrelativistic particle in a one-dimensional box. Doing so yields

$$E(n) = \int_0^L \mathrm{sgn}(x-n)|\psi_1(x)|^2 dx = 1 - \frac{2n}{L} + \frac{\sin(2\pi n/L)}{\pi}, \tag{20}$$

where $\psi_1(n) = \sqrt{2/L}\sin(\pi n/L)$ is the ground-state wave function of a spinon. The result is shown in Fig. 8(a) as a dashed curve. While the agreement is already rather good, further improvements can be made, as explained below.

Just to the left of the $m=1/2$ plateau, the ladder contains a few spinons with spin $\Delta S^z=-1/2$ each. Because the first and last rungs still remain in the triplet state, the ground state of a ladder with an even number of rungs L and spin $S^z = L/2-p$ contains $r=2p+1$ spinons. At low concentrations r/L the spinons can be treated as ideal fermions.[19] The envelope of the staggered magnetization $E(n)$ is the expectation value $\langle(-1)^{s(n)}\rangle$, where $s(n)$ is the number of spinons to the left of rung n. The average is taken over the ground state of nonrelativistic fermions occupying the first r levels with wave functions $\psi_k(n) = \sqrt{2/L}\sin(\pi k n/L)$. The result for r spinons is

$$E(n) = \det S(n). \tag{21}$$

The $r\times r$ matrix $S(n)$ has elements

$$S_{ij}(n) = \int_0^L \mathrm{sgn}(x-n)\psi_i^*(x)\psi_j(x)dx, \tag{22}$$

where $\psi_i(x)$ are the spinon wave functions of the *occupied* states: $i=1\cdots r$. See Appendix D for a derivation. The numerical data and the theoretical curve for $S^z=L/2-1$ (3 spinons) are shown in Fig. 8(b).

The agreement between the theoretical curve and the numerical data can be further improved by taking into account the spin $\Delta S^z=-1/2$ carried by the domain walls,

$$\langle S_n^z \rangle = \frac{1}{2} - \frac{(-1)^n E(n)}{2} - \frac{1}{2}\sum_{k=1}^{r} |\psi_k(n)|^2, \tag{23}$$

and by figuring in the reduction of staggered magnetization by quantum fluctuations. The leading effect is a virtual exchange of a singlet and triplet on neighboring rungs. This process increases the energy by J (the strength of triplet repulsion), has the matrix element $\delta J/2 \ll J$, and thus can be treated as a small perturbation. To a leading order in $\delta J/J$ we find a simple reduction of the envelope $E(n)$ by the factor $1-(\delta J/J)^2$. See Appendix E for details.

Close to the plateau when the spinon gas is dilute, the deviation of the magnetization density from 1/2 is expected to be proportional to $|H-H_{c2}|^{1/2}$, in complete analogy to the magnon case (18). However, the magnetization curve (Fig. 4) evidently remains linear almost all the way to H_{c2}, with only a hint of an upturn right next to the plateau. A possible reason for this behavior could be the narrowness of the critical region near H_{c2} where the spinons can be treated as noninteracting fermions. One argument in favor of this interpretation is the relative smallness of the square-root term whose amplitude is $\pi^{-1}|\Delta S^z|^{3/2}|2m^*|^{1/2}$. In comparison to the magnons, the spinons have a reduced spin ΔS^z and a smaller mass m^* (by a factor of 4 to leading order in δJ). We also note that magnetization curves of an easy-axis XXZ chain[17] show a similar trend: the square-root term near the Néel-ordered state is relatively small.

3. $0<m<1$: *a Luttinger liquid*

The gapless phase in the field range $H_{c1}<H<H_{c2}$ is a Luttinger liquid[18] with continuously varying critical indices. The critical properties of the ladder are expected to be similar to those of the easy-axis XXZ chain in the gapless regime $H_{\min}<|H_{xxz}|<H_{\max}$ in which the compressibility exponent K decreases monotonically between 1 (dilute magnons) and 1/4 (dilute spinons).[22]

The compressibility exponent can be determined by examining the Friedel oscillations in local magnetization $\langle S_n^z \rangle$ induced by the presence of the ends.[23] In a ladder of length L, the leading behavior of magnetization away from the ends is

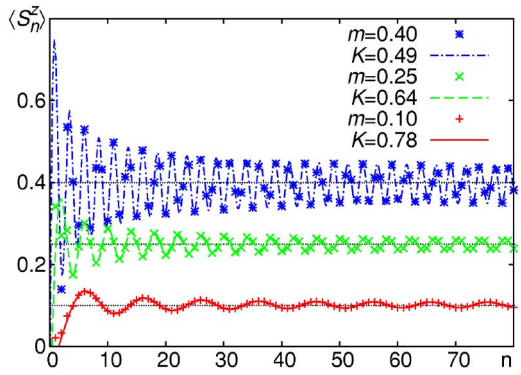

FIG. 10. (Color online) Friedel oscillations of the local magnetization $\langle S_n^z \rangle$ for three values of average magnetization m. The lines are best fits to the theoretical curves (24). The fits were performed in the range $n_0 \leqslant n \leqslant L+1-n_0$ with $n_0=5$.

$$\langle S_n^z \rangle \sim \text{const} + \frac{a \cos(2\pi m n + \beta)}{[L \sin(\pi n/L)]^K}, \tag{24}$$

where m is the concentration of magnons and β is a phase shift. Fits of the numerical data to this form are shown in Fig. 10 for a ladder of length $L=160$. The extracted exponent K is shown in Fig. 11 as a function of the magnetization m. While there is a weak dependence on the short-range cutoff n_0, the trend is consistent with a monotonic decrease of K from 1 to 1/4.

IV. INFLUENCE OF ANISOTROPY

Experimentally accessible spin systems are almost inevitably anisotropic. While an anisotropy may be small numerically, it may induce qualitative changes in the system's behavior because it lowers the symmetry. This is particularly important in the vicinity of a critical point or phase: the presence of a symmetry-breaking term can change the nature of a phase transition or even completely eliminate it. While the physical causes of anisotropies can vary, close to a critical point their influence on the system can be expressed in terms of a few relevant physical variables. A well-known

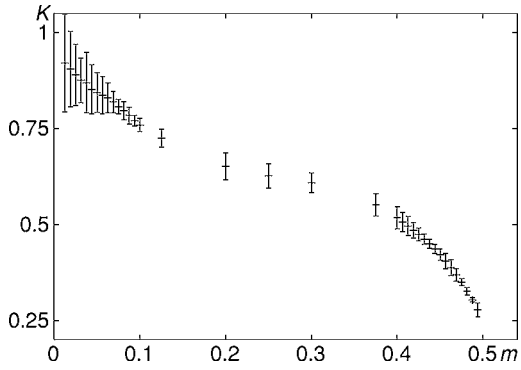

FIG. 11. The compressibility exponent K as a function of magnetization m in the gapless phase between fields H_{c1} and H_{c2}. The error bars reflect the range of K values obtained for different choices of the short-range cutoff n_0.

example is the breaking of the axial $O(2)$ symmetry of a spin chain under an external magnetic field by the anisotropic Dzyaloshinskii-Moriya (DM) interaction. The action of the DM term is equivalent to that of a weak staggered field transverse to the applied one.[12,13]

A staggered field is uniquely defined in bipartite antiferromagnets. A frustrated antiferromagnet can be partitioned into two sublattices in more than one way. Accordingly, several staggered fields can be introduced in such cases.[24] Three staggered fields are potentially relevant to our ladder:

$$V = \sum_{n=1}^{L} [h_{\pi 0}(-1)^n S_n^x + h_{0\pi} D_n^x + h_{\pi\pi}(-1)^n D_n^x]. \tag{25}$$

(The fields are labeled by their Fourier indices.) The most relevant perturbation at a phase transition is that which couples directly to an order parameter. In our case ($J_1 < J_2 < J$), the "condensate" at H_{c1} has the wave vector $(0,\pi)$. The staggered field $h_{0\pi}$ coupled to it breaks down the $O(2)$ symmetry completely. In its presence, the quantum phase transition at H_{c1} is expected to become a crossover. The other two staggered fields couple to the square of the order parameter, generating an easy-axis anisotropy along either x or y directions and thus lowering the symmetry from $O(2)$ down to Z_2. In the absence of the more relevant staggered field $h_{0\pi}$, the critical point at H_{c1} will be preserved, but the universality class is expected to change from commensurate-incommensurate to Ising.

Our numerical work is focused on the influence of the staggered field $h_{0\pi}$. (In what follows we drop the wave-vector index.) We choose its amplitude to be proportional to the magnitude of the external field, as happens with the Dzyaloshinskii-Moriya interaction:[12,13] $h=cH$. The anisotropy coefficient c is varied between 0 and 0.1. Figure 12 shows the magnetization $m(H)$ and energy gap $\Delta(H)$ for $c=0.03$ for several lengths of the ladder L.

The introduction of the transverse field destroys the magnetization plateaus: the spin projection S^z is no longer conserved. However, the fate of the quantum critical points is different for the transitions out of the integer (H_{c1}) and fractional (H_{c2} and H_{c3}) magnetization plateaux. A complete lack of finite-size effects near H_{c1} is a good indication that the magnon condensation point H_{c1} has become a crossover. In contrast, near the points of spinon condensation, H_{c2} and H_{c3}, the energy gap Δ is still sensitive to the system size, indicating that the critical points survive the introduction of anisotropy.

A. Anisotropy and magnon condensation

As noted above, the introduction of even a weak staggered field ($h=0.03H$) completely suppresses finite-size effects in ladders of length $L=50$ and more. This is fully consistent with the scaling theory of Bose condensation in the presence of a symmetry-breaking transverse field.[7,25] A finite transverse field $h=cH$ generates a finite correlation length $\xi \propto \Delta^{-1} \propto c^{-4/5}$. Evidently, for $c=0.03$ we have $\xi \lesssim 50$, so that ladders with $L \geqslant 50$ are already in the thermodynamic limit.

The magnetization and energy gap for several values of anisotropy c are shown in Figs. 13(a) and 13(b). The data are

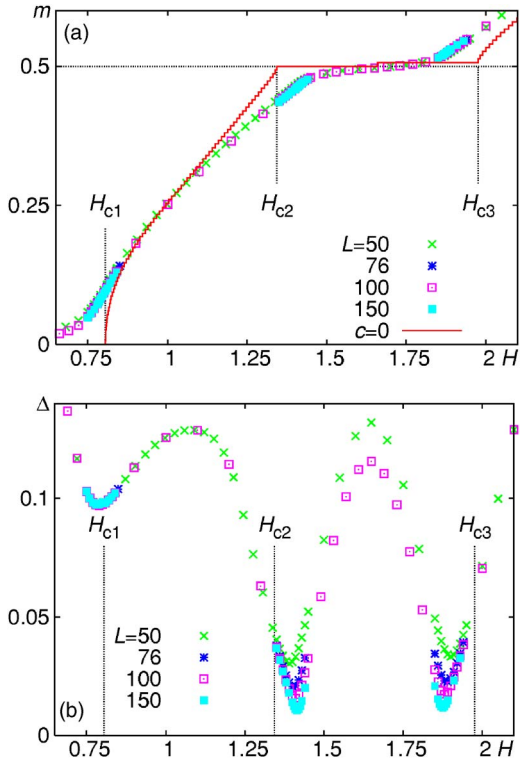

FIG. 12. (Color online) Finite-size effects on magnetization (a) and energy gap (b) in the presence of a small anisotropy $c=0.03$. The solid line shows $m(H)$ for $c=0$ and $L=150$. The dotted lines mark the critical fields H_{c1}, H_{c2}, and H_{c3}. L is the length of the ladders.

in agreement with the scaling theory.[25] As shown in Fig. 13(c), the energy gap obeys the scaling law

$$\Delta(H-H_{c1},c)=c^{4/5}\Phi[(H-H_{c1})c^{-4/5}]. \tag{26}$$

Exactly at H_{c1} the energy gap is proportional to $c^{4/5}$, while the magnetization $m(H_{c1})\propto c^{2/5}$.

B. Anisotropy and spinon condensation

In contrast, for the same value of anisotropy, strong finite-size effects are observed near the spinon condensation points H_{c2} and H_{c3} (Fig. 12). This indicates that the quantum phase transitions survive the introduction of the staggered transverse field $h_{0\pi}$.

The more robust nature of the spinon transitions can be traced to the spontaneous breaking of a discrete lattice symmetry at the fractional plateau: the two ground states (Fig. 3) break any symmetry transformation that exchanges even and odd lattice rungs. The addition of the staggered field $h_{0\pi}$ keeps some of these symmetries intact (e.g., the translation by one lattice spacing), so that the Hamiltonian remains more symmetric than the ground states. In other words, the Z_2 translational order remains in what used to be the fractional plateau. Restoration of the Z_2 symmetry at H_{c2} (and H_{c3}) requires a phase transition, whether the transverse field $h_{0\pi}$ is present or not.

The difference can also be understood by looking at the effect of the staggered field on the elementary excitations of

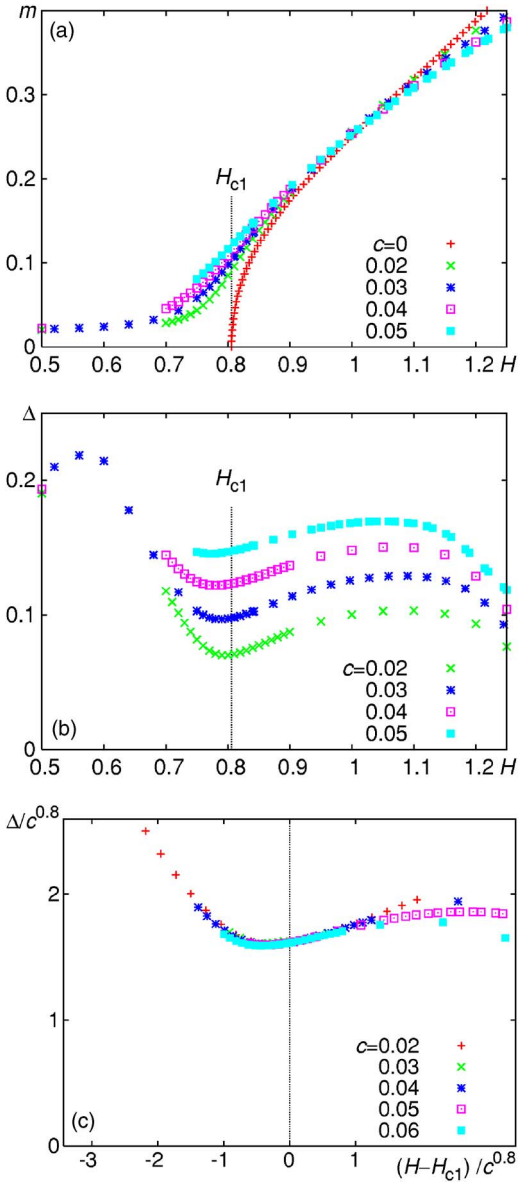

FIG. 13. (Color online) Magnetization (a) and energy gap (b) near H_{c1} for several values of the anisotropy parameter c (see text). (c) Scaling of the energy gap near H_{c1}. The dotted line shows the location of the critical field.

the integer and fractional plateaus. By coupling to operators D_n^+ and D_n^-, the staggered field adds or subtracts angular momentum 1. As a result, it creates or destroys single magnons (spin 1) at H_{c1} and H_{c4} but pairs of spinons (spin 1/2) at H_{c2} and H_{c3}. A plausible effective Hamiltonian for the spinons with low momenta near the critical point in a weak transverse field would be

$$\mathcal{H}_{xxz}=\sum_p [(p^2/2m-\mu)a_p^\dagger a_p+ivp(a_p^\dagger a_{-p}^\dagger-a_{-p}a_p)], \tag{27}$$

where p is the spinon momentum, $\mu\propto H-H_{c2}$ is the chemical potential, and $v\propto h_{0\pi}$ is a pairing field. The energy gap behaves as follows:

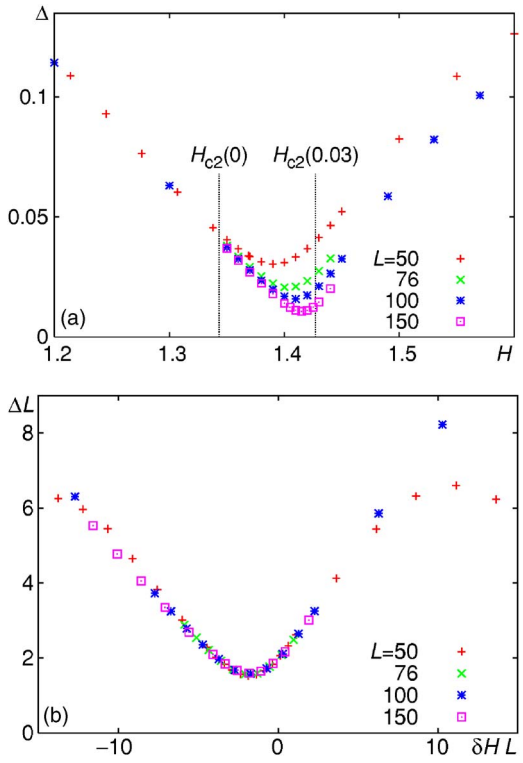

FIG. 14. (Color online) Finite-size scaling of the energy gap near the critical field H_{c2} in the presence of finite anisotropy $c=0.03$. The dotted line marks the location of H_{c2} in the absence of anisotropy.

$$\Delta = \begin{cases} |\mu|, & \text{if } \mu < mv^2, \\ \sqrt{mv^2(2\mu + mv^2)}, & \text{if } \mu > mv^2. \end{cases} \tag{28}$$

The spinon condensation in 1+1 dimensions is thus similar to the commensurate-incommensurate transitions in two-dimensional statistical mechanics.[26] In the absence of the transverse field $h_{0\pi}$, it belongs to the metal-insulator (Pokrovsky-Talapov) universality class. Switching on the field converts the transition to the Ising universality class.

We have verified that, for a fixed anisotropy c, the finite-size scaling of the energy gap is consistent with the Ising transition in 1+1 dimensions:

$$\Delta(\delta H, L) = L^{-1} f(\delta H L), \tag{29}$$

where $\delta H = H - H_{c2}(c)$. Note that the critical field depends on the anisotropy parameter c. The scaling for $c=0.03$ is shown in Fig. 14.

As the anisotropy constant c increases, the critical fields H_{c2} and H_{c3} shift towards each other, see Fig. 15. The two fields merge and the ordered phase disappears at a modest value of the anisotropy $c \approx 0.06$. Above this value of c, the ground state is nondegenerate and does not break the translational symmetry for any value of H.

Ideally, we would have liked to verify the universal scaling at the quantum critical point $H=H_{c2}$, $c=0$, $1/L=0$, just like we did at the magnon condensation point H_{c1}. In this case, one expects to observe a crossover from the Ising critical behavior to that of the Pokrovsky-Talapov class. As can

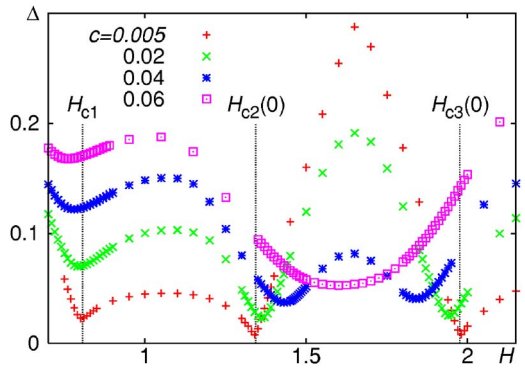

FIG. 15. (Color online) Energy gap as a function of the field for several values of anisotropy c in a ladder of fixed length $L=50$. The dotted lines mark the critical fields H_{c1}, H_{c2}, and H_{c3}.

be inferred from Eq. (28), the energy gap is expected to cross over from $|H-H_{c2}|$ on the gapped side to $|H-H_{c2}|^{1/2}$ in the formerly gapless region. We have not been able to observe this crossover. This failure may be related to the narrowness of the region where the spinons can be treated as noninteracting fermions with a quadratic energy dispersion. (See Sec. III B 2.) To observe the crossover, one probably needs to work with a very small anisotropy c (we went down to 5×10^{-4}) and rather long ladders to avoid finite-size effects.

V. DISCUSSION

We have presented a model of a one-dimensional quantum antiferromagnet in external magnetic field. The system exhibits both integer and fractional magnetization plateaus. The quantum critical points at the ends of an integer plateau are well-described by the Bose condensation of magnons. At low densities, the condensing magnons behave as hard-core bosons or, alternatively, can be described as weakly interacting fermions. The introduction of a weak anisotropy fully breaking the $O(2)$ symmetry of the model replaces the quantum phase transition with a crossover. In contrast, a fractional magnetization plateau breaks a Z_2 (Ising-like) symmetry of the lattice and ends in a condensation of spinons—domain walls in the Z_2 order parameter. Magnetization patterns at low spinon densities are explained by modeling the spinons as free fermions. The introduction of a weak anisotropy preserves the Z_2 symmetry of the model. As a result, the quantum phase transition at the end of a fractional plateau survives.

This difference between integer and fractional plateaux is expected to show up in the properties of quantum antiferromagnets in higher dimensions as well. In that respect, $SrCu_2(BO_3)_2$, a physical realization of the Shastry-Sutherland model, is a prominent candidate, with plateaus at $m=1/8$, $m=1/4$, and $m=1/3$ that spontaneously break the translational symmetry of the crystal.[27,28] It is well-established by now that there are significant Dzyaloshinskii-Moriya interactions in that compound[29] and that a gap persists in the region between the $m=0$ and $m=1/8$ plateaus, and closes (or has a deep minimum) before entering the $m=1/8$ plateau. This behavior is reminiscent of the gap behav-

ior we found for the frustrated ladder. Given the pecularities of the triplet kinetic energy in the Shastry-Sutherland model,[30,31] the extension to that case of the ideas developed in the present paper is far from trivial.

ACKNOWLEDGMENTS

We gratefully acknowledge discussions with F. D. M. Haldane, A. Läuchli, S. Miyahara, M. Oshikawa, O. Tretiakov, and M. Troyer. This work was supported in part by the U.S. National Science Foundation Grants No. DMR-0348679 and DMR-0412956, by the Swiss National Fund, and by MaNEP.

APPENDIX A: THE SPIN OPERATORS ACTING ON A RUNG

There are four states on each rung, which decompose into a singlet and a triplet under spin $\mathbf{S}=\mathbf{S}_1+\mathbf{S}_2$. We denote the singlet as $|s\rangle$, and the $S_z=1,0,-1$ components of the triplet as $|+\rangle$, $|0\rangle$, and $|-\rangle$, respectively. The spin difference operator $\mathbf{D}=\mathbf{S}_1-\mathbf{S}_2$ acts as follows:

$$D^z|s\rangle=|0\rangle,\quad D^z|0\rangle=|s\rangle,\quad D^z|\pm\rangle=0,$$

$$D^\pm|\mp\rangle=\pm\sqrt{2}|s\rangle,\quad D^\pm|s\rangle=\pm\sqrt{2}|\pm\rangle,$$

$$D^\pm|\pm\rangle=0,\quad D^\pm|0\rangle=0, \tag{A1}$$

where $D^\pm=D^x\pm iD^y$.

APPENDIX B: SPINON ENERGY AT $O(\delta J^2)$

To compute the second-order correction to the *XXZ* Hamiltonian, one needs the action of $\mathcal{H}_2$ on states comprised of singlets and $S_z=1$ triplets. It follows from Eq. (A1) that $\mathbf{D}_n\cdot\mathbf{D}_{n+1}$ acts nontrivially only on nearest-neighbor pairs of singlets, giving for one pair

$$\mathcal{H}_2|ss\rangle=\frac{\delta J}{2}(|+-\rangle+|-+\rangle-|00\rangle). \tag{B1}$$

One can now do second-order perturbation theory to compute the correction to the *XXZ* Hamiltonian coming from annihilating and creating pairs of triplets out of the adjacent singlet states. Since these pairs are created between other magnons when the system is near the $m=1/2$ plateau, the perturbation theory requires the diagonalization of $\mathcal{H}_1$ on a length-4 chain of triplets. Calling the resultant states ψ_i and their $\mathcal{H}_1$ eigenvalues λ_i, one finds that the shift in energy coming from having singlets on adjacent sites is

$$E^{(2)}_{ss}=\sum_i\frac{|\langle\psi_i|\mathcal{H}_2|+ss+\rangle|^2}{-2-\lambda_i}=C(J)\delta J^2, \tag{B2}$$

where

$$C=\frac{1/20}{-2}+\frac{1/5}{-2+J}+\frac{(5-\sqrt{21})/20}{-2-\frac{-1+\sqrt{21}}{2}J}+\frac{(5+\sqrt{21})/20}{-2+\frac{1+\sqrt{21}}{2}J}. \tag{B3}$$

At $J=0.625$ we obtain $C=-2.026$. The largest contribution comes from the last term where the excited state lies rather close to the spinon (an energy difference of 0.255).

APPENDIX C: MAGNON ENERGY AT $O(\delta J^2)$

In Sec. III B 1, we have determined the inverse magnon mass to leading order in δJ. Here we evaluate the next-order correction in the limit of well-separated energy scales (3). To this end, we consider the state of the ladder with a single $S^z=+1$ triplet in the background of singlet states. For $\delta J=0$ any such state is an eigenstate of the Hamiltonian $\mathcal{H}_0+\mathcal{H}_1$ (2). The first-order correction in δJ induces the hopping of the magnon to the next site with the amplitude $\delta J/2$, yielding an inverse mass $1/m^*=|\delta J|$.

Second-order corrections to the magnon kinetic energy include hopping through intermediate states with additional magnons. An example of such a process is shown in Fig. 5. Such a process involves the creation of a pair of magnons with total spin 0 next to the original magnon and the subsequent destruction of a magnon pair by the perturbation term $\mathcal{H}_2$. Since both of these events have the amplitude $O(\delta J)$, we may treat the dynamics of the intermediate 3-magnon state using the zeroth-order Hamiltonian $\mathcal{H}_0+\mathcal{H}_1$. At that level, the 3-magnon composite is immobile. However, it has some internal dynamics: the spins of the individual magnons S^z_n may fluctuate. We therefore first discuss the internal dynamics of the composite.

A 3-magnon composite with the total spin $\Delta S^z=+1$ has six internal states:

$$|-++\rangle,\ |+-+\rangle,\ |++-\rangle,\ |+00\rangle,\ |0+0\rangle,\ |00+\rangle. \tag{C1}$$

In this basis, $\mathcal{H}_0=3-H$, while

$$\mathcal{H}_1=J\begin{pmatrix}0&0&0&0&0&1\\0&-2&0&1&0&1\\0&0&0&1&0&0\\0&1&1&0&1&0\\0&0&0&1&0&1\\1&1&0&0&1&0\end{pmatrix}. \tag{C2}$$

The lowest energy composite state is close to that shown in Fig. 5(b) and has the energy $3-H-3J$. The energy gap between the magnon and the 3-magnon composite is $\Delta_1=2-3J$. Our numerical studies were done on a system with $J=0.625$, which yields a gap $\Delta_1=0.125$, comparable to the perturbation strength $\delta J=0.15$. It is therefore not surprising that the leading-order result for the magnon mass was not reliable.

To evaluate corrections at $O(\delta J^2)$, we examine the hybridization of the magnon a_n with the 3-magnon composites $c_{\gamma n}$ (where $\gamma=1\cdots6$ is the internal index):

$$\mathcal{H}_{\text{magnon}} = \sum_n (\delta J/2)(a_n^\dagger a_{n-1} + \text{H.c.}) + \sum_n \sum_{\gamma=1}^{6} \Delta_\gamma c_{\gamma n}^\dagger c_{\gamma n} + \sum_n \sum_{\gamma=1}^{6} [c_{\gamma n}^\dagger (\lambda_\gamma a_{n+1} + \rho_\gamma a_{n-1}) + \text{H.c.}], \quad \text{(C3)}$$

where λ_γ and ρ_γ are matrix elements involved in creating a 3-magnon composite centered on the left or on the right of the magnon:

$$\lambda_\gamma = \langle s | c_{\gamma n} \mathcal{H}_2 a_{n+1}^\dagger | s \rangle, \quad \rho_\gamma = \langle s | c_{\gamma n} \mathcal{H}_2 a_{n-1}^\dagger | s \rangle, \quad \text{(C4)}$$

where $|s\rangle$ is the all-singlet vacuum state. Elimination of the hybridization term to $O(\delta J)$ via a unitary transformation

$$c_{\gamma n} \mapsto c_{\gamma n} - (\rho_\gamma a_{n-1} + \lambda_\gamma a_{n+1})/\Delta_\gamma \quad \text{(C5)}$$

generates an additional magnon hopping term at $O(\delta J^2)$:

$$-\sum_{\gamma=1}^{6} \frac{\rho_\gamma \lambda_\gamma}{\Delta_\gamma} \sum_n a_{n-1}^\dagger a_{n+1} + \text{H.c.} \quad \text{(C6)}$$

This yields the inverse magnon mass

$$1/m^* = |\delta J| + 8 \sum_{\gamma=1}^{6} \frac{\rho_\gamma \lambda_\gamma}{\Delta_\gamma} = |\delta J| + 2\left(\frac{1}{6} - \frac{1}{2-J} + \frac{5}{3(2-3J)}\right)\delta J^2. \quad \text{(C7)}$$

The calculation is simplified because the one-magnon state only couples to three of the six composite states. For our choice of the coupling constants, the second-order correction to the inverse mass (0.575) is almost four times as large as the first-order term (0.15) thanks to the small energy gap between 1- and 3-magnon states.

The same unitary transformation allows us to determine the shift of the magnon energy at this order:

$$\Delta\epsilon_{1,1} = -\left(\frac{1}{6} + \frac{5}{3(2-3J)}\right)\delta J^2 + E_{\text{Casimir}}. \quad \text{(C8)}$$

The second term comes from the effect of the magnon on the vacuum. The Hamiltonian term $\mathcal{H}_2$ creates virtual excitations in the form of two triplets on adjacent rungs. These virtual processes shift the vacuum energy by

$$\Delta E_0 = \sum_i \frac{|\langle p_i | \mathcal{H}_2 | s \rangle|^2}{-2+2J} = \frac{-3L\delta J^2}{4(2-2J)}, \quad \text{(C9)}$$

where $\langle p_i \rangle$ is the intermediate state (B1) with two triplets next to each other. In the presence of a magnon the vacuum fluctuations are suppressed in the immediate vicinity of the magnon. The factor L in Eq. (C9) is replaced with $L-4$, increasing the energy of the 1-magnon state by the Casimir term in Eq. (C8)

$$E_{\text{Casimir}} = 3\delta J^2/2(1-J). \quad \text{(C10)}$$

The second-order correction to the magnon condensation field is then

$$\Delta H_{c1} = \Delta\epsilon_{1,1} = -9.5\delta J^2 = -0.214. \quad \text{(C11)}$$

Again, because of the small energy gap to excited states, the second-order correction to H_{c1} exceeds the first-order one (-0.15) and does not improve the agreement with the numerics.

APPENDIX D: ENVELOPE OF STAGGERED MAGNETIZATION

In this section we derive the expression for the envelope of the staggered magnetization (21). We work in the continuum limit and treat spinons as noninteracting fermions in a box with $0 < x < L$. Since each spinon serves as a domain wall, the envelope $E(x)$ is found by averaging the operator

$$\hat{E}(x) = \prod_{i=1}^{r} \text{sgn}(x_i - x) \quad \text{(D1)}$$

over the (fully antisymmetric) wave function of r spinons

$$\Psi(x_1 \cdots x_r) = \frac{1}{\sqrt{r!}} \sum_{\{k\}} \varepsilon_{\{k\}} \prod_{i=1}^{r} \psi_{k_i}(x_i), \quad \text{(D2)}$$

where $\varepsilon_{\{k\}} = \varepsilon_{k_1 \cdots k_r}$ is the fully antisymmetric tensor with $\varepsilon_{12\cdots r} = +1$.

The averaging yields

$$E(x) = \frac{1}{r!} \sum_{\{k\}} \sum_{\{l\}} \varepsilon_{\{k\}} \varepsilon_{\{l\}} \prod_{i=1}^{r} S_{k_i l_i}(x) \quad \text{(D3)}$$

with the matrix $S_{ij}(x)$ defined in Eq. (22). It can be simplified by noting that $\varepsilon_{\{k\}}\varepsilon_{\{l\}} = (-1)^P$, where P is the permutation that maps $\{k\}$ into $\{l\}$. Shifting from the sum over $\{k\}$ and $\{l\} = P(\{k\})$ to a sum over $\{k\}$ and P allows the sum over $\{k\}$ to be performed trivially to obtain

$$E(x) = \sum_P (-1)^P \prod_{i=1}^{r} S_{iP_i}(x) = \det S(x). \quad \text{(D4)}$$

APPENDIX E: REDUCTION OF STAGGERED MAGNETIZATION

The domain wall magnetization envelope will be reduced by the presence of quantum fluctuations. The leading order effect is the creation and subsequent annihilation of a pair of domain walls due to the interchange of a singlet and a triplet on neighboring sites. The domain wall Hamiltonian for the *XXZ* chain is[32]

$$H = \sum_j \frac{J}{2} c_j^\dagger c_j + \frac{\delta J}{2}(1 - c_j^\dagger c_j)(c_{j+1}^\dagger c_{j-1} + c_{j+1} c_{j-1} + \text{H.c.}), \quad \text{(E1)}$$

where the c operators obey fermionic commutation relations. We shall ignore the quartic terms in this Hamiltonian in the approximation of low spinon density.

Since these domain walls represent boundaries between the Néel states with $S_n^z=(-1)^n/2$ and $(-1)^{n+1}/2$, the expectation value of the spin on rung n in a state $|\psi\rangle$ is

$$\langle S_n^z\rangle = \frac{(-1)^n}{2}\langle\psi|E_n|\psi\rangle \tag{E2}$$

in addition to the spin carried by the spinons themselves. Here $E_n=(-1)^{s(n)}$, where $s(n)$ is the number of spinons to the left of rung n.

The spinon-number changing terms in the Hamiltonian can be eliminated to lowest order in $\epsilon=\delta J/J$ by the unitary transformation

$$c_n \mapsto e^{-B}c_n e^{B}, \quad B=\frac{\epsilon}{2}\sum_j c_{j+1}^\dagger c_{j-1}^\dagger - \text{H.c.} \tag{E3}$$

We can write the eigenstates of H as $|\psi\rangle=e^B|\tilde{\psi}\rangle$, where $|\tilde{\psi}\rangle$ is an eigenstate of $e^{-B}He^B$ with definite spinon number. We now have that

$$\begin{aligned} S_n &= \frac{(-1)^n}{2}\langle\tilde{\psi}|e^{-B}E_n e^{B}|\tilde{\psi}\rangle \\ &= \frac{(-1)^n}{2}\langle\tilde{\psi}|E_n - [B,E_n] + \frac{1}{2}[B,E_n] + \cdots|\tilde{\psi}\rangle \\ &= \frac{(-1)^n}{2}\langle\tilde{\psi}|E_n + \frac{\epsilon^2}{8}\Bigg[\sum_j (c_{j+1}^\dagger c_{j-1}^\dagger + c_{j+1}c_{j-1}), \\ &\quad \Bigg[\sum_i (c_{i+1}^\dagger c_{i-1}^\dagger + c_{i+1}c_{i-1}), E_n\Bigg]\Bigg]|\tilde{\psi}\rangle \\ &= \frac{(-1)^n}{2}(1-\epsilon^2)\langle\tilde{\psi}|E_n|\tilde{\psi}\rangle + O(1/L) + O(\epsilon^3). \end{aligned} \tag{E4}$$

Here we have used the relation

$$c_m E_n = \mathrm{sgn}(m-n)E_n c_m \tag{E5}$$

and its adjoint. Note that the first-order term vanishes because the operator $[B,E_n]$ includes a net change in the number of spinons. The $O(1/L)$ piece arises from terms in the commutator proportional to the spinon density operator. The second order term is independent of the number of spinons. Hence the leading effect of the quantum fluctuations is to reduce the value of the staggered magnetization by a factor of $1-(\delta J/J)^2$.

[1] S. Sachdev, *Quantum Phase Transitions* (Cambridge University Press, Cambridge, England, 2001).
[2] G. R. Stewart, Rev. Mod. Phys. **56**, 755 (1984).
[3] D. Bitko, T. F. Rosenbaum, and G. Aeppli, Phys. Rev. Lett. **77**, 940 (1996).
[4] M. Greiner, O. Mandel, T. Esslinger, T. W. Hänsch, and I. Bloch, Nature (London) **415**, 39 (2002).
[5] I. Affleck, Phys. Rev. B **41**, 6697 (1990); **43**, 3215 (1991).
[6] T. Giamarchi and A. M. Tsvelik, Phys. Rev. B **59**, 11398 (1999).
[7] M. P. A. Fisher, P. B. Weichman, G. Grinstein, and D. S. Fisher, Phys. Rev. B **40**, 546 (1989).
[8] M. Oshikawa, M. Yamanaka, and I. Affleck, Phys. Rev. Lett. **78**, 1984 (1997).
[9] P. Fendley, K. Sengupta, and S. Sachdev, Phys. Rev. B **69**, 075106 (2004).
[10] P. Lecheminant and E. Orignac, Phys. Rev. B **69**, 174409 (2004).
[11] F. H. L. Essler and I. Affleck, J. Stat. Mech.: Theory Exp. (2004) P12006.
[12] Q. Xia and P. S. Riseborough, J. Appl. Phys. **63**, 4141 (1988).
[13] M. Oshikawa and I. Affleck, Phys. Rev. Lett. **79**, 2883 (1997).
[14] F. Mila, Eur. Phys. J. B **6**, 201 (1998).
[15] D. C. Cabra, A. Honecker, and P. Pujol, Phys. Rev. Lett. **79**, 5126 (1997).
[16] A. Honecker, F. Mila, and M. Troyer, Eur. Phys. J. B **15**, 227 (2000).
[17] C. N. Yang and C. P. Yang, Phys. Rev. **151**, 258 (1967).
[18] F. D. M. Haldane, J. Phys. C **14**, 2585 (1981).
[19] M. Fowler and M. W. Puga, Phys. Rev. B **18**, 421 (1978).
[20] S. R. White, Phys. Rev. Lett. **69**, 2863 (1992).
[21] R. M. Noack and S. R. Manmana, in *Lectures on the Physics of Highly Correlated Electron Systems IX: Ninth Training Course in the Physics of Correlated Electron Systems and High-Tc Superconductors* edited by A. Avekka and F. Mancini AIP Conf. Proc. No. 789 (AIP, Melville, NY, 2005), p. 93.
[22] F. D. M. Haldane, Phys. Rev. Lett. **45**, 1358 (1980).
[23] S. R. White, I. Affleck, and D. J. Scalapino, Phys. Rev. B **65**, 165122 (2002).
[24] S. Sachdev, Phys. Rev. B **45**, 12377 (1992).
[25] J.-B. Fouet, O. Tchernyshyov, and F. Mila, Phys. Rev. B **70**, 174427 (2004).
[26] M. den Nijs, in *Phase Transitions and Critical Phenomena*, edited by C. Domb and J. L. Lebowitz (Academic, New York, 1988), Vol. 12.
[27] H. Kageyama, K. Yoshimura, R. Stern, N. V. Mushnikov, K. Onizuka, M. Kato, K. Kosuge, C. P. Slichter, T. Goto, and Y. Ueda, Phys. Rev. Lett. **82**, 3168 (1999).
[28] K. Kodama, M. Takigawa, M. Horvatic, C. Berthier, H. Kageyama, Y. Ueda, S. Miyahara, F. Becca, and F. Mila, Science **298**, 395 (2002).
[29] K. Kodama, S. Miyahara, M. Takigawa, M. Horvatic, C. Berthier, F. Mila, K. Kageyama, and Y. Ueda, J. Phys.: Condens. Matter **17**, L61 (2005).
[30] S. Miyahara and K. Ueda, J. Phys.: Condens. Matter **15**, R327 (2003).
[31] R. Bendjama, B. Kumar, and F. Mila, Phys. Rev. Lett. **95**, 110406 (2005).
[32] G. Gómez-Santos, Phys. Rev. B **41**, 6788 (1990).